Journal of Integrative Neuroscience

J. Integr. Neurosci. **2024**; 23(1): 22
https://doi.org/10.31083/j.jin2301022

Original Research

Influence of Anodal tDCS on the Brain Functional Networks and Muscle Synergy of Hand Movements

Sijia Chen[1], Zhizeng Luo[1,*], Jianjun Lai[2,*]

[1]Institute of Intelligent Control and Robotics Hangzhou Dianzi University, 310018 Hangzhou, Zhejiang, China
[2]Department of Radiation Oncology, Zhejiang Hospital, 310013 Hangzhou, Zhejiang, China
*Correspondence: luo@hdu.edu.cn (Zhizeng Luo); 385806945@qq.com (Jianjun Lai)
Academic Editor: Yoshihiro Noda
Submitted: 9 August 2023 Revised: 16 September 2023 Accepted: 21 September 2023 Published: 22 January 2024

Abstract

Background: Transcranial direct current stimulation (tDCS) is a non-invasive technique that has demonstrated potential in modulating cortical neuron excitability. The objective of this paper is to investigate the effects of tDCS on characteristic parameters of brain functional networks and muscle synergy, as well as to explore its potential for enhancing motor performance. **Methods**: By applying different durations of tDCS on the motor cortex of the brain, the 32-lead electroencephalogram (EEG) of the cerebral cortex and 4-lead electromyography (EMG) signals of the right forearm were collected for 4 typical hand movements which are commonly used in rehabilitation training, including right-hand finger flexion, finger extension, wrist flexion, and wrist extension. **Results**: The study showed that tDCS can enhance the brain's electrical activity in the beta band of the C3 node of the cerebral cortex during hand movements. Furthermore, the structure of muscle synergy remains unaltered; however, the associated muscle activity is amplified ($p < 0.05$). **Conclusions**: Based on the study results, it can be inferred that tDCS enhances the control strength between the motor area of the cerebral cortex and the muscles during hand movements.

Keywords: EEG; EMG; tDCS; brain functional networks; muscle synergy

1. Introduction

Stroke is the leading cause of motor impairments on a global scale [1]. Despite numerous interventions, a considerable number of post-stroke individuals encounter difficulties in executing movements due to impaired motor functions in both upper and lower limbs, significantly impacting their daily living activities [2].

In recent years, substantial progress has been achieved in both research and practical implementation of non-invasive brain stimulation techniques, including repetitive transcranial magnetic stimulation (rTMS) and transcranial direct current stimulation (tDCS). Empirical evidence [3] suggests that rTMS possesses a commendable safety profile to modulate cortical excitability, potentially enhancing overall cognitive performance. Adverse effects such as cutaneous tingling or headaches may arise in some cases. Compared to rTMS, tDCS is considered a more suitable therapeutic tool due to its greater convenience of application [4]; tDCS equipment is relatively portable and can be carried by one person. It entails the application of a low-intensity electrical current, typically around 2 mA, to a targeted cerebral area utilizing 2 or more electrodes. This electrical current elicits alterations at subthreshold levels, thereby influencing the likelihood of neural firing when a neuron is subjected to input from another neuron. As a non-invasive, low-intensity intervention that modulates neuronal activity in the cerebral cortex, tDCS possesses the capability to alter the spontaneous synaptic activity of neurons [4]. Previous studies [5,6] have demonstrated the influence of tDCS on the excitability of the spinal cord by modulating the motor and visual cortex. tDCS can be divided into anodal and cathodal stimulation, where anodal stimulation can increase cortical excitability, and cathodal stimulation can decrease cortical excitability [7,8]. In practice, tDCS offers numerous advantages, including a small stimulation current, high safety, adjustable polarity and position, and ease of operation, providing a new solution for motor function rehabilitation. To date, the available empirical data is insufficient to support the notion that multiple sessions of active tDCS pose greater harm to subjects when compared to sham tDCS, based on the parameters tested thus far [9,10]. Indeed, Zaghi *et al*. [11] have confirmed that when tDCS is combined with occupational therapy in stroke patients, it can significantly improve fine motor function. Andrés Molero-Chamizo *et al*. [12] found that the motor cortex excitability changes induced by tDCS can improve motor responses. Numerous investigations have extensively reported the linkage between anodal stimulation of the primary motor cortex (M1) and enhancements in various behavioral aspects, including executive function and rowing performance [13], acquisition of novel skills [14,15], as well as motor imagery and finger tapping reaction time (RT) [16]. There are many similar qualitative studies on tDCS, such as literature [17–19], etc. Although there are many studies on the effect of tDCS, there are relatively few studies on the mechanism of its stimulation.

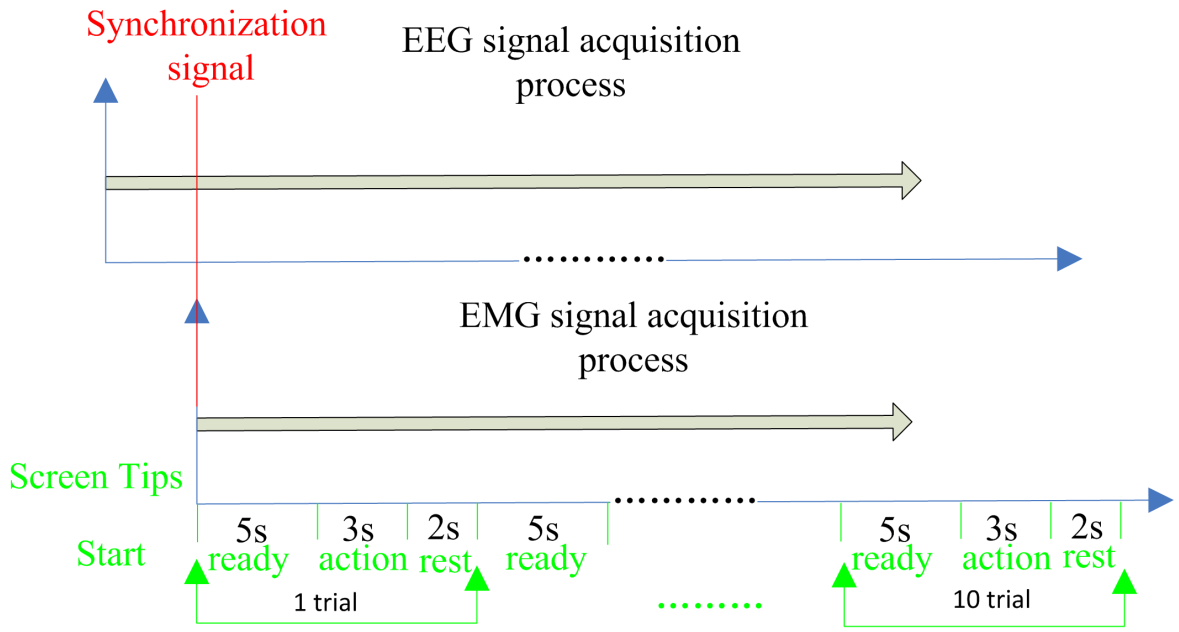

Fig. 1. Schematic diagram of EEG and EMG acquisition. EEG, electroencephalogram; EMG, electromyography.

The Fugl-Meyer Assessment (FMA) [20] serves as a stroke-specific, performance-based impairment index that is widely employed to evaluate limb movement ability in stroke patients. To date, numerous studies [21,22] have confirmed that the FMA scores of stroke patients are significantly improved after tDCS interventions, and these findings further support the notion that tDCS has the potential to enhance limb movement abilities in the body. Nevertheless, the predominant body of research has mainly concentrated on examining the impact of tDCS on the enhancement of limb function among stroke patients. However, there has been limited exploration of the underlying mechanism of tDCS.

This paper mainly studies the brain function network [23] and muscle synergy [24] of tDCS on hand movements to preliminarily explore the mechanism of the influence of tDCS on human movement ability. The brain function network is a valuable indicator of the abnormality of the connection between different regions of the cerebral cortex. Muscle synergy is the activation of a group of muscles to contribute to a particular movement. Nicolas J. Beuchat *et al.* [25] were able to successfully decode muscle synergies from EEG. The study [26] indicated cortical correlates of muscle synergy activation, possibly suggesting that the cortex is involved in hierarchical control of locomotor muscle activity through muscle synergies.

In this research, we enlisted healthy participants to acquire EEG and EMG signals while executing 4 typical hand movements (namely finger flexion, finger extension, wrist flexion, and wrist extension). The study participants underwent tDCS prior to engaging in these hand movements with varying durations (0 minutes, 5 minutes, and 15 minutes). An analysis of characteristic parameters related to brain functional networks and muscle synergies was performed using the specified experimental conditions and resultant data. The primary objective of this investigation was to assess the influence of tDCS duration, specifically on brain functional networks and muscle synergies during hand movements.

2. Materials and Methods

In this experiment, the Trigno Wireless System EMG acquisition system of DELSYS company (Boston, MA, USA) was applied to collect EMG signals from 4 channels. The Trigno system offers high-quality EMG signal acquisition, wireless convenience, and multi-channel recording capabilities. Flexor carpi ulnaris (FCU), extensor digitorum (ED), extensor carpi radialis (ECR), flexor digitorum (FD), and the acquisition frequency were all set to 1000 Hz (The main frequency range of EMG signal is 20~450 Hz). The positions of these 4 groups of muscles are mainly determined according to the human muscle distribution map when the hand makes a fist. Concurrently, 32 channels of EEG signals were collected using the NeuSen W series wireless EEG acquisition system (Neuracle Inc., Beijing, China) of Brightcom Corporation based on the 10–20 International System. The NeuSen W series system offers high-resolution EEG acquisition, wireless freedom, and real-time monitoring and control features. To facilitate the subsequent segmentation of data segments, the acquisition frequency of EEG was also set to 1000 Hz. Primary Motor Cortex (M1) is a specific area of the cerebral cortex located in the frontal lobe area in front of the central gyrus (Central Sulcus). M1 is considered to be the area mainly responsible for motor control, of which C3 is mainly responsible for the right limb movement, and C4 is mainly

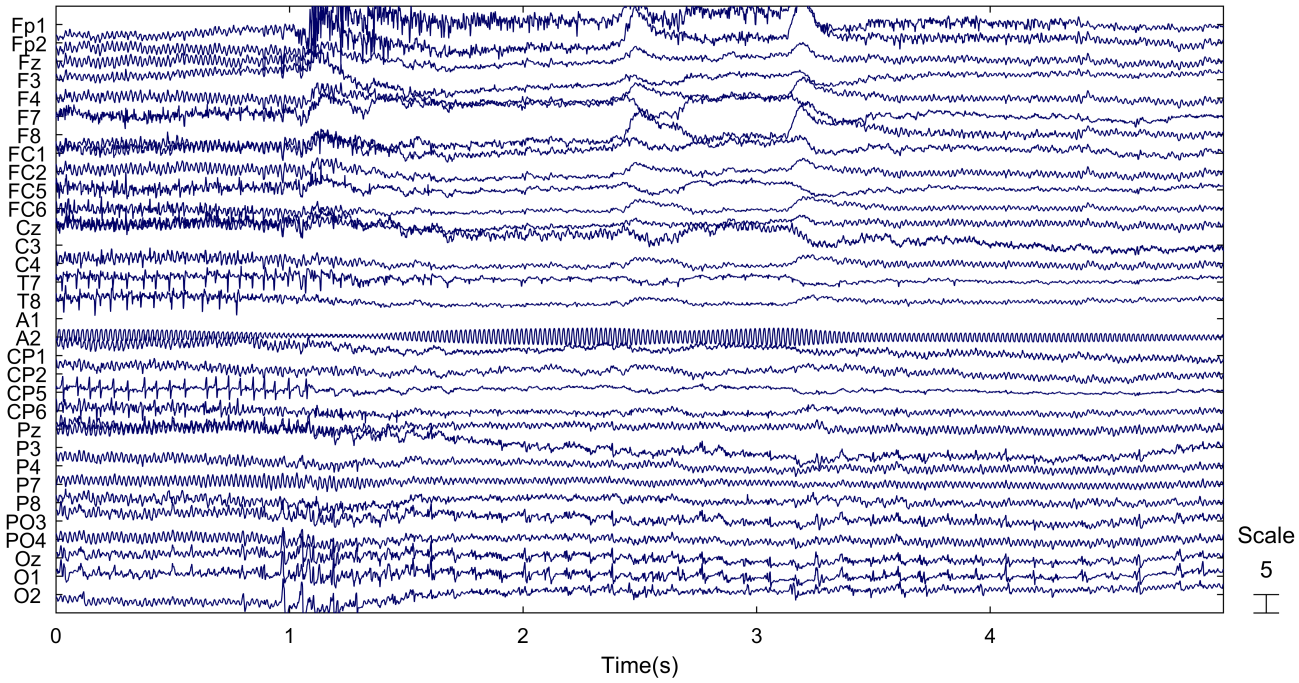

Fig. 2. Partial EEG signals during finger flexion in the sham group.

responsible for left limb movement. Therefore, in the study of the effect of tDCS on exercise, the stimulation site was predominantly located at C3/C4 [27]. In this experiment, the primary focus was on right limb movements; thus, the stimulation point is C3, with a stimulation current of 2 mA. The electrode size is π cm^2 (circular). The anode is placed at C3, and the cathode is placed on the upper side of the right orbit (FP2, frontopolar area 2). In order to ensure the reliability of the experimental data, the stimulation mode adopts a double-blind method.

In addition, here is a brief definition of 4 kinds of hand movements:

Finger Flexion: Finger flexion refers to the bending of the fingers, typically towards the palm, resulting in the curling of the finger joints.

Finger Extension: Finger extension refers to the opening of the fingers.

Wrist Flexion: Wrist flexion involves bending the wrist joint towards the palm side of the hand.

Wrist Extension: Wrist extension involves bending the wrist joint in the opposite direction, away from the palm side of the hand.

The experimental protocol was executed utilizing Eprime-2.0 software (Carnegie Mellon University, Pittsburgh, PST; Pittsburgh, PA, USA), which facilitated the design and implementation of psychological experiments. Eprime offers a user-friendly interface for experiment design and data collection, supporting various stimulus types such as text, images, audio, and video. The process of EMG acquisition was triggered by the synchronization signal, which was sent by the Eprime. The specific process is depicted in Fig. 1. Initially, EEG signal collection was commenced, and when Eprime displayed "Start", the experimenter initiated EMG signal collection by clicking the corresponding button. Simultaneously, this action prompted Eprime to transmit a synchronization signal to the EEG collection software, and put a synchronization label on the EEG signal. Subsequently, the screen displayed the word "ready", allowing participants a 5-second preparation period. The hand movement duration was set to 3 seconds, followed by a relaxation period of approximately 2 seconds. Each set of movements was iterated 10 times. Since there is a latency between participants perceiving the on-screen prompts and initiating the corresponding actions, the initiation point for each action did not precisely coincide with the 5th second of each action cycle. Consequently, the subsequent selected data segments could not be intercepted according to a fixed time point. Nevertheless, the EEG and EMG signals share the same acquisition frequency; they are synchronized from the initial signal synchronization point. Moreover, the amplitude of the EMG signal clearly delineated the temporal duration of the action. Thus, the subsequent segmentation of action synchronization segments for the EEG and EMG data relied on the EMG data, serving as a reliable indicator for identifying the periods of action. Specifically, when the magnitude of the EMG signal exceeds a specific threshold, that point was designated as the commencement of a particular segment with a fixed data length. Subsequently, a specific data segment was omitted, and the subsequent initiation point was identified anew. To mitigate the impact of noise on this process, manual verification was conducted afterward.

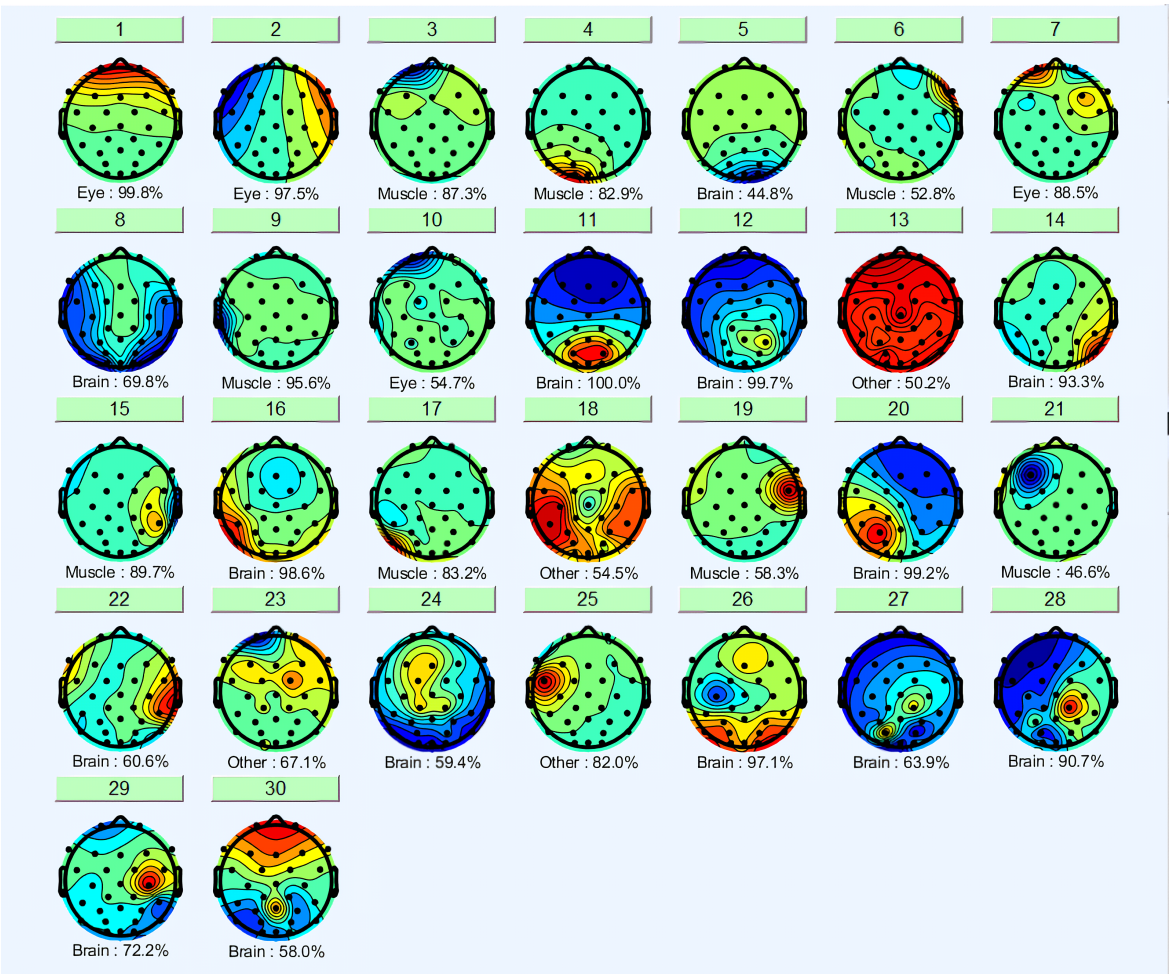

Fig. 3. Schematic diagram for the specific categories of 30 independent components decomposed by ICA of EEG signal during finger flexion in the sham group. ICA, Independent Component Analysis.

The study involved 30 healthy adult participants, comprising 16 males and 14 females, with ages ranging from 24–32. All participants were right-handed, as determined by the short form of the Edinburgh Handedness Inventory [28]. They had no history of neurological diseases and possessed equivalent levels of education. Before the start of the experiment, none of the participants took any drugs or food that affected the central nervous system. The stimulator of tDCS is the Neustim of Brightcom Corporation (Changzhou, JiangSu, China), which allows for flexible adjustment of stimulation position and parameters. The participants were randomly divided into 3 groups, each containing 10 individuals: the sham group, which did not receive tDCS; the experimental group, stimulated with tDCS for 5 minutes and 15 minutes. Specifically, the 30 participants were assigned serial numbers from 1 to 30, and simultaneously, 10 group numbers labeled ‘0’, ‘1’, and ‘2’ were randomly assigned to these 30 serial numbers. In this assignment, ‘0’ signified the sham group, ‘1’ means tDCS for 5 minutes, and ‘2’ means tDCS for 15 minutes. The sham group is primarily to eliminate the influence of volunteers’ psychology and other factors on the experimental results. To minimize the influence of electrooculographic artifacts, other unrelated muscle groups in the body, and the noise signals generated by electrode movement during the EEG acquisition process, the participants were instructed to maintain a relaxed posture, sit facing the screen with their gaze directed upward, and endeavor to minimize head movements and blinking throughout the experiment. Additionally, proper electrode preparation was ensured by cleaning the scalp with an appropriate conductive gel or saline solution, reducing impedance and enhancing signal quality.

The MATLAB R2018bB version (MathWorks, Natick, MA, USA) used to analyze and process the data in this experiment is R2018bB, and the EEGlab version is V2021 (University of California, Oakland, CA, USA).

2.1 Signal Processing

2.1.1 Signal Preprocessing

Initially, EEGlab was employed to import the EEG data and visualize the distribution of the 32-channel EEG signals. Extraneous electrodes were excluded from subsequent analysis. Specifically, electrodes A1 and A2, typi-

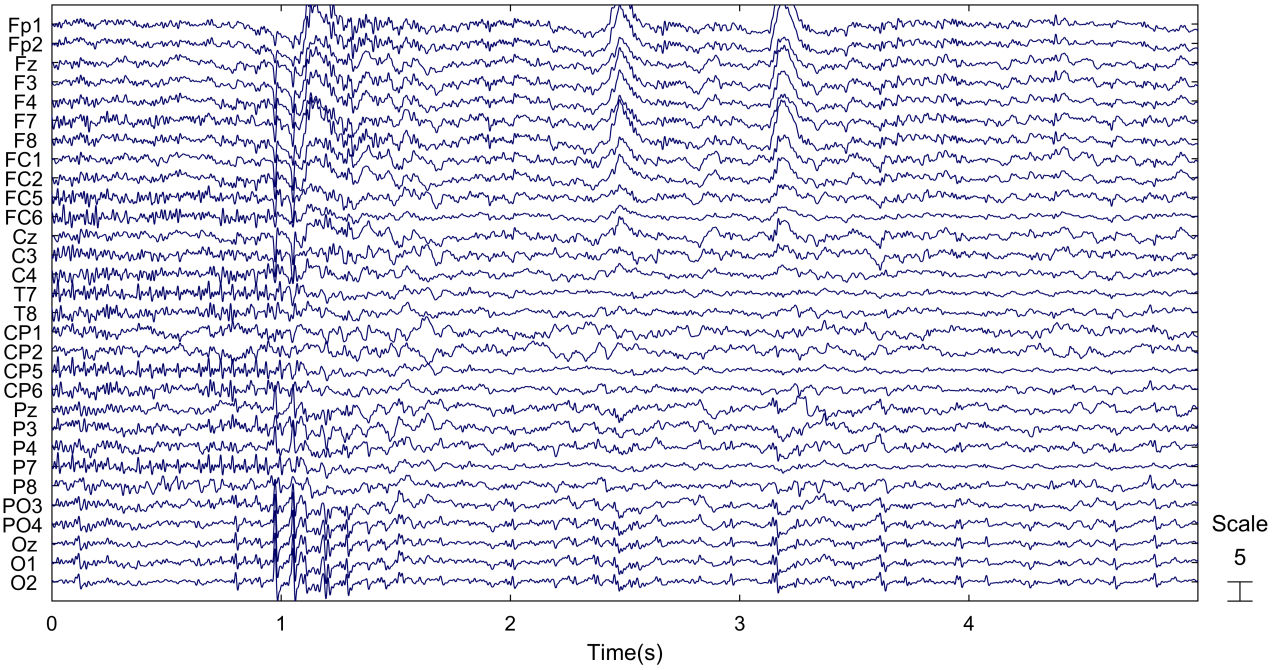

Fig. 4. Signals after denoising EEG during finger flexion in the sham group.

cally proximate to the earlobe and commonly used as reference electrodes, were omitted from the experiment setup. In this study, the value of the reference electrode is the mean value of all effective electrodes; therefore, electrodes A1 and A2 were not included. Fig. 2 illustrates the raw EEG data collected. During the experiment, electrodes A1 and A2 were not very close to the position of the earlobe, resulting in abnormal values for these 2 channels.

Given the susceptibility of the signal acquisition process to 50 Hz power frequency interference, coupled with the inherent frequency characteristics of EEG and EMG signals, this study employed a data processing methodology to mitigate the impact of power frequency interference in the acquired signals. To elaborate, the EEGlab toolbox was employed to remove power frequency interference from the EEG signals, followed by preprocessing using a bandpass filter ranging from 0.1–80 Hz. Concurrently, the EMG signal was also processed to mitigate the power frequency interference, with preprocessing involving the application of a bandpass filter ranging from 30 to 450 Hz.

Despite the assumption made in the experimental protocol, achieving ideal conditions in actual experiments is unattainable. The initial assumption was that participants would minimize eye blinks and extraneous muscle movements that could disrupt EEG signals. Consequently, for signal preprocessing, it is imperative to address the elimination of noise components, such as electrooculogram (EOG), in preparation for subsequent analysis and processing. Furthermore, this experiment entailed the collection of EEG signals from 30 channels. However, not all EEG channels were pertinent to hand movements during the experiment. Hence, it is essential to mitigate the EEG noise originating from non-hand movements (e.g., blinking, nodding, opening mouth, etc., any action that may generate brain noise). This measure proves advantageous in reducing the workload associated with subsequent data analysis.

Independent component analysis (ICA) can be effectively applied to EEG signals through the EEGlab toolbox. As an exceptional blind source separation algorithm, ICA is often used in research on brain source localization [29]. It is capable of separating the artifacts in EEG signals [30,31], including such noises as muscles, blinks, or eye movements, without affecting the disturbed EEG data. In EEGlab, there are a variety of ICA algorithms available to choose from. There are many ICA classification algorithms [32] in the EEGlab toolbox, combined with reference [33] and own tests, adaptive mixture of independent component analyzers (AMICA) [34] was applied due to the better results of separation for multi-channel EEG data. The ICA algorithm is capable only of separating different independent components from the EEG data, which means it is ineffective in identifying the specific source of the corresponding components. Thus, it is necessary to rely on ICLabel [35] for classifying and identifying the independent components separated by ICA. After separating the independent components, it identifies one of the 7 categories, including Brain, Muscle, Eye, Heart, Line Noise, Channel Noise, and others, before an estimate of percentage probability is given. The number of independent components decomposed by ICA corresponds to the number of EEG channels. Fig. 3 depicts the specific categories of the 30 independent components decomposed by the EEG signal of flexion before tDCS. The other category predominantly comprises unidentified noise and other unidentified EEG components. The percentage

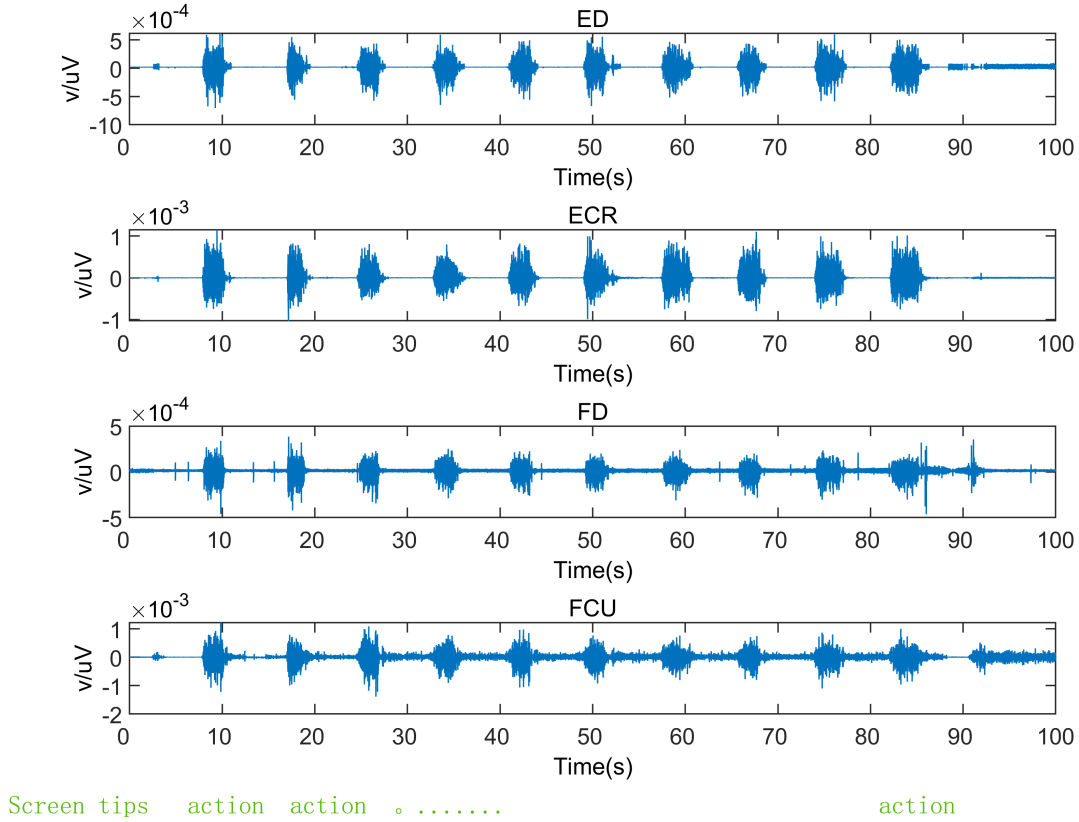

Fig. 5. Signal after EMG denoising during finger flexion in the sham group. FCU, Flexor carpi ulnaris; ED, extensor digitorum; ECR, extensor carpi radialis; FD, flexor digitorum.

values beneath each subgraph represent the probability associated with each component. It can be seen that there is a lot of noise in the EEG signal, such as eye electricity, myoelectricity, etc. For example, components 1 and 2 are electro-ocular noise, and predicted probabilities are 0.998 and 0.975, respectively. These high probabilities suggest that the volunteers may have blinked frequently during data collection. Noise is typically considered when the probability exceeds a certain threshold, which is commonly set between 0.5 and 0.9 [36,37]. In order to remove the noise component in the EEG as much as possible and retain the effective EEG signal as much as possible without unintended deletion, this paper sets the threshold to 0.5; that is, the noise component with a higher probability than 0.5 was eliminated, according to the classification results of ICLabel. According to the above rules, the components 1, 2, 3, 4, 6, 7, 9, 10, 13, 15, 17, 20, 18, 19, 23, and 25 in Fig. 3 are all proposed, and Fig. 4 is the noise removal the signal restoration diagram after component. It can be seen that compared with Fig. 2, the EEG signal is significantly improved.

2.1.2 Signal Segmentation

The EEG signal's synchronization marker is synchronized with the start of EMG signal acquisition, ensuring consistency in the time domain. Furthermore, the frequency of data collection remains consistent between the EMG and EEG signals. Fig. 5 depicts the EMG signal recorded during finger flexion in the sham group. The initiation and termination of each motion can be clearly observed, which makes the amplitude of the EMG signal applicable as a criterion to segment the EMG and EEG data simultaneously. Although in the design of the experiment process, the duration of the action is 3 seconds, but by observing the electromyogram, it can be found that the duration of many actions is about 2 seconds. This may be due to the relatively high intensity of the action, and the long duration is more tiring. In order to ensure that the signal data corresponding to the intercepted period is complete action data, this study selected a 1.5-second data segment for each action cycle, equivalent to 1500 data points following the onset of each action. Besides, each segment in this dataset consisted of 300 sampling points. That is to say, there was a time window of 300 milliseconds, and the moving step was comprised of 100 sampling points.

2.2 Analysis of Characteristic Parameters of Brain Functional Network

The EEG signal is representative of a time-domain waveform, with a primary focus on analyzing variations in amplitude over time. This temporal analysis approach [38] offers superior temporal precision and accuracy in comparison to frequency-domain analysis. However, the sole

reliance on time-domain analysis may not adequately capture the entirety of information present in the EEG signal. To extract a broader range of information, the EEG signal can be segmented into sub-signals of varying frequency ranges through frequency-domain analysis, thereby allowing for subsequent investigations. Both of these analytical approaches are employed in this paper.

The human brain can be conceptualized as an intricately complex system. The interaction among distinct brain regions is fundamental to the realization of brain function, and the construction of the brain function network involves combining the EEG timing signals of distributed brain regions with graph theory. The primary steps of constructing the brain function network in this study are as follows:

(1) Select network nodes. In this study, the area where each scalp electrode patch is located is defined as a node.

(2) EEG signal preprocessing. Initially, a bandpass filtering spanning 0.1–80 Hz is applied to eliminate extraneous noise interference. Subsequently, the independent component analysis method is employed to reconstruct the signal after removing artifacts such as oculograph, eye drift, and head movement. Finally, the EEG signal to be studied is decomposed into 5 frequency bands.

(3) Correlation analysis between nodes. Various methods for correlation analysis exist, including cross-correlation, mutual information, and phase synchronization index. In this paper, the cross-correlation analysis is selected, the EEG time series of the 2 channels are expressed, and the cross-correlation coefficient is calculated using the following expression:

$$R_{xy} = \frac{n \sum_{i=1,j=1}^{n} x_i y_j - \left(\sum_{i=1}^{n} x_i\right)\left(\sum_{j=1}^{n} y_j\right)}{\sqrt{n \sum_{i=1}^{n} x_i^2 - \left(\sum_{i=1}^{n} x_i\right)^2}\sqrt{n \sum_{j=1}^{n} y_j^2 - \left(\sum_{j=1}^{n} y_j\right)^2}} \quad (1)$$

Among them i j represent the sampling points of the EEG signal and n represent the total sampling number. The value R_{xy} is between 0 and 1; a value of 0 indicates that there is no correlation between the signals, and a value of 1 indicates that the signals are completely correlated.

(4) Threshold selection (T). Following the above procedures, a connection coefficient matrix can be obtained, which can be transformed into a binary matrix after selecting an appropriate threshold, and the topology of the brain functional network can be derived from this matrix. The correlations of neural oscillations in delta, theta, alpha, beta, and gamma bands were different, so different thresholds were selected to construct the brain function network. Consistent with prior literature [39], this study opted for the thresholds of 0.38, 0.56, 0.63, 0.43, and 0.32 for the respective frequency bands.

Upon completing the construction of the brain function network, characteristic parameters of the brain function network are extracted using a complex network measurement method. The similarities and disparities in network characteristic parameters before and after tDCS can elucidate the impact of stimulation on the internal connectivity characteristics of the brain. In this study, the degree and average clustering coefficient are chosen as characteristic parameters to analyze the influence mechanism of tDCS on typical hand movements.

(1) Degrees. The degree of node i represents the sum of the number of connections between this node and other nodes in the network. The degree value provides an intuitive indication of a node's importance within the network. The node with a higher degree value is, in a sense, the node of the network core node. The degree value of node i is expressed as follows:

$$D_{\mathrm{i}} = \sum_{j=1}^{N} h_{ij} \quad (2)$$

where h_{ij} represents the connection between nodes i and j; N represents the number of nodes.

(2) Average clustering coefficient. The clustering coefficient measures the connection tightness of nodes in a complex network, expressed as the possibility of interconnection between a certain node and other nodes. Assume that a node i has k_i neighbor nodes, and there are actually e_i connection edges between the network midpoint and these neighbor nodes. At the same time, it can be calculated that the maximum number of possible connection edges between point e_i and its neighbor nodes is $k_i\left(k_i-1\right)/2$, then the clustering coefficient C_i of node i can be defined as:

$$C_i = \frac{2e_i}{k_i\left(k_i-1\right)} \quad (3)$$

The average clustering coefficient C is expressed as the average value of the clustering coefficients of all nodes in the network, which can evaluate the characteristics of the network as a whole. The formula is as follows:

$$C = \frac{1}{N}\sum_{i=1}^{N} C_i \quad (4)$$

The value range of the clustering coefficient is between 0 and 1, indicating that there are no nodes connected to each other in the current network, indicating that any 2 nodes in the network have a connection relationship.

2.3 Muscle Synergies

Muscle synergy analysis is primarily employed to investigate how the central nervous system orchestrates muscles in a modular way to achieve coordinated movement [40]. It offers a simplified depiction of intricate mecha-

Table 1. After different durations of tDCS, the data of the first four channels with the largest EEG average power during hand movements.

Electrode \ tDCS duration	Average power		
	0 minutes	5 minutes	15 minutes
C3	10.31 ± 0.61	11.61 ± 1.02*	12.53 ± 0.98*
P3	8.53 ± 1.58	8.82 ± 0.73	9.19 ± 0.24*
F3	8.41 ± 0.63	8.89 ± 1.05*	9.55 ± 0.84*
Cz	6.75 ± 0.62	6.53 ± 0.89	6.91 ± 1.02

The values are presented as the mean ± standard deviation. The values are presented as the mean ± standard deviation. *indicates that there is a significant difference in the current group in comparison to the sham group (0 minutes) ($p < 0.05$). tDCS, Transcranial direct current stimulation.

nisms of motor control. This theory was initially proposed by Bernstein *et al*. [41] in 1967, contending that the central nervous system does not always perform real-time calculations to optimally control diverse muscle groups for generating a desired movement. The muscle synergy theory proposes that a complete limb movement results from the combination of several inherent minimum basic muscle group movement units, and this superimposition mechanism entails a form of collaboration. The study of muscle synergy may help clarify neurological disorders caused by the central nervous system, including stroke, cerebral palsy, spinal cord injury, Parkinson's disease, etc.

The non-negative matrix factorization (NNMF) algorithm [42] was utilized to extract muscle synergies from EMG signals.

$$M(t) = \sum_{i=1}^{n} (W_i \times H_i(t)) + E \tag{5}$$

Where M(t) is the L*N EMG signals matrix (L muscles and N number of samples), W is the L*S synergy matrix (S number of synergies), and H is the S*N coefficient matrix. The weight matrix W comprises the weights of individual muscles for the corresponding synergies, while the activation matrix H denotes the level of activation or utilization of each synergy for force generation. Under this framework, the contribution of an individual muscle to the task performed can be expressed as a linear combination of the product of its weight Wi and the corresponding activation coefficient Hi(t).

In muscle synergy analysis, it becomes imperative to determine the value of S, which represents the number of muscle synergies. The guiding principle for determining this value is to minimize the number of synergies while ensuring that the reconstructed EMG signal closely approximates the original signal. The method used for this purpose is the variance accounted for (VAF) index [43], which is given by Eqn. 6. Here, X represents the matrix formed by the envelope-extracted EMG signal, A represents the activation matrix, and C represents the synergy matrix, both of which are obtained using the non-negative matrix factorization (NMF) method. The larger the number of muscle synergies, the closer the reconstructed EMG signal will be to the original signal. Typically, the value of S corresponding to a VAF greater than 0.9 is chosen as the number of muscle synergies.

$$VAF = 1 - \frac{\left\| \left(M(t) - \sum_{i=1}^{s} (W(i) * H(i)) \right)^2 \right\|}{\|M(t)\|^2} \tag{6}$$

In addition to comparing the number of muscle synergies, the similarity of muscle synergies can also be compared using various methods, including Pearson's correlation coefficient, circular cross-correlation coefficient [44], and cosine similarity (CS) [45]. These methods can be used to compare the similarity between different muscle synergy structure matrices or activation coefficient matrix vectors. In this article, cosine similarity is used to measure the similarity of muscle synergy structure matrix vectors. The formula for cosine similarity is as follows:

$$CS = \cos(\theta) = \frac{W_i * W_j}{\|W_i\| \, \|W_j\|} \tag{7}$$

2.4 Statistical Analysis

The data were analyzed by SPSS version 24.0 for Windows (SPSS Inc, Chicago, IL, USA). All of the participants were tested for normality through the Shapiro-Wilk test. p values were derived from 2-way analysis of variance (ANOVA). The effects of several groups of dependent variables on stimulation results, such as stimulation time and electrode, frequency band and hand movements, and hand movements and stimulation time, were examined, respectively. Multiple comparison post-hoc tests were also conducted when the ANOVA found a significant effect and used the Bonferroni correction for multiple comparisons [46]. For all comparisons, $p < 0.05$ was considered statistically significant.

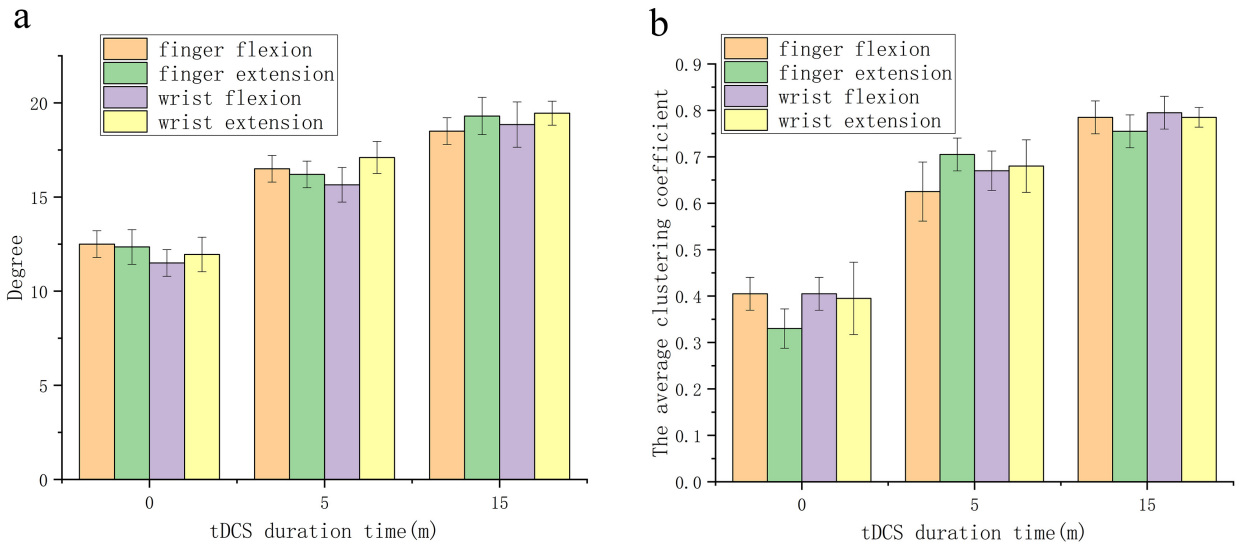

Fig. 6. The characteristic parameters of the brain functional networks during four typical hand movements under different tDCS durations, the degree of C3 nodes (a), average clustering coefficient (b).

3. Results

Table 1 presents the data for the 4 channels with the largest EEG average power levels during hand movements following various durations of tDCS. The power spectral density of each channel was computed using the Welch method, which relies on the fast fourier transform (FFT) algorithm and the Hanning window [47]. A window length of 1 second and an overlap rate of 50% were employed for the calculations, and then the results were averaged to get average power. It can be seen that the EEG activity of C3, P3, and F3 channels is the strongest when the hand is moving. Compared with the sham group (stimulation of 0 minute), the average power of the C3 node was significantly increased under different stimulation durations, the P3 node was significantly increased after 15 minutes of stimulation, and the F3 node was significantly increased after 5 minutes. It can be seen that the selection of the location of the anode stimulation of tDCS determines the area affected by the cerebral cortex. This table reflects the significant difference between tDCS stimulation and sham group. In addition, through statistical comparative analysis between 5-minute and 15-minute stimulation, it was found that there were significant differences in the stimulation results of C3, P3, and F3.

Table 2 presents the mean degree values of EEG-C3 nodes derived from the topological structure data of the binarized brain functional network in the sham group. The analysis revealed that compared with other frequency bands, the beta band of the EEG had a significant difference ($p < 0.05$) in all kinds of hand movements. Simultaneously, in analyzing the data of the experimental group, we found similar conclusions. This finding indicates that during hand movements, the beta band signal of EEG played a major role. This finding is also consistent with the traditional understanding that the beta band signal is one of the EEG signals closely associated with limb movement. Furthermore, there was a significant difference in the alpha band in the finger extension movement, but it did not appear in other movements. This discrepancy may be attributed to the potential incompleteness of noise reduction utilizing the EEGlab tool.

Fig. 6 depicts the degree of C3 and the average clustering coefficients during 4 typical hand movements under varying durations of tDCS durations. When combined with Fig. 6b, it becomes evident that tDCS significantly enhanced the activity of the C3 node, and it was positively correlated with the duration of tDCS stimulation. Simultaneously, the average clustering coefficient in Fig. 6b reflected the compactness of different cerebral cortex regions, and tDCS significantly increased the average clustering coefficient of the brain functional network, indicating its potential to augment cerebral cortex activity during limb movement, which has great guiding significance for the rehabilitation exercise of patients with movement disorders. Additionally, it was observed that the average clustering coefficients of tDCS for 5 minutes were significantly improved, while the effect of 15 minutes of tDCS was not very obvious. This may be because the effect of tDCS would be saturated within a certain period, or it may be due to the effect of tDCS. The effect was mainly reflected in the brain area near the C3 node.

Fig. 7 presents a comparison of VAF curves between the sham and control groups of participants. For S = 3, the VAF values surpassed the threshold (0.9) across all evaluated conditions. After undergoing tDCS, the EMG signals reconstructed using muscle synergy were found to be greater than those obtained from the sham group under the same muscle synergy conditions.

Table 2. The mean value of the degree of EEG-C3 nodes obtained from the topological structure data of the binarized brain functional network in the sham group.

Movements / EEG band	Mean node degree of EEG-C3				
	delta	theta	alpha	beta	gamma
Finger flexion	9.01 ± 0.31	6.33 ± 1.28	8.91 ± 1.03*	13.25 ± 0.65*	6.21 ± 2.08
Finger extension	8.41 ± 2.42	8.42 ± 1.73	8.81 ± 1.15	12.53 ± 0.69*	3.53 ± 3.12
Wrist flexion	8.3 ± 1.48	6.9 ± 0.24	8.3 ± 2.34	13.61 ± 1.15*	2.46 ± 2.52
Wrist extension	9.21 ± 2.15	6.72 ± 2.57	7.45 ± 2.06	12.42 ± 1.56*	3.46 ± 1.63

The values are presented as the mean ± standard deviation. *indicates that there is a significant difference between the current frequency band and all other frequency bands ($p < 0.05$).

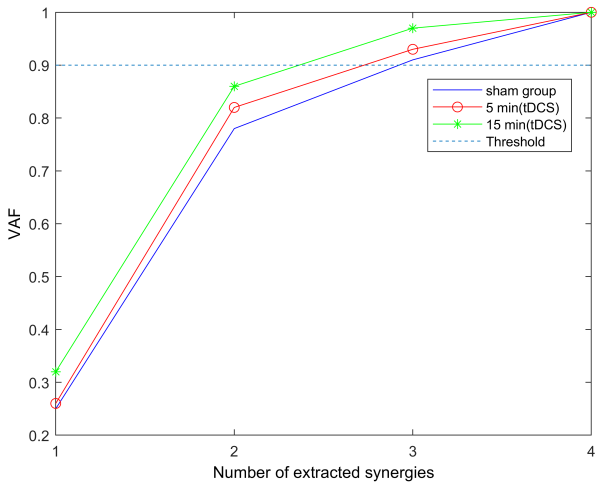

Fig. 7. Comparing VAF curves between the sham and control groups of participants. VAF, Variance accounted for.

Table 3 serves as a summary table of presenting comparisons among muscular synergy vectors for each hand movement. The CS index across different experimental groups is found to be quite similar. This observation suggests that the structure of muscle synergy represented by matrix W has undergone minimal changes, and W represents the relative weight of each muscle group, which means that tDCS will not change the cooperative relationship between each muscle group during hand movements, but tDCS will change the muscle synergistic activation matrix H. Post-hoc analyses revealed that there were no significant differences between different experimental groups under all hand movements. Combined with the brain function network parameters and the previous analysis, tDCS has been found to significantly augment the neural activity of the C3 node in the human brain, and this effect exhibits a positive correlation with the duration of tDCS. It can be concluded that tDCS mainly enhanced the EEG signal of the C3 node and thus stimulated greater muscle activity.

4. Discussion

Anodal tDCS has the potential to enhance cortical activity in the areas of anodal stimulation. By analyzing the characteristic parameters of the brain functional networks,

Table 3. Summary table of comparisons among muscular synergy vectors for each exercise.

Movements / Groups	CS (cosine similarity)		
	(S-5)	(S-15)	(5–15)
Finger flexion	0.96 ± 0.05	0.97 ± 0.02	0.96 ± 0.06
Finger extension	0.98 ± 0.04	0.96 ± 0.03	0.97 ± 0.02
Wrist flexion	0.98 ± 0.06	0.97 ± 0.01	0.98 ± 0.04
Wrist extension	0.93 ± 0.03	0.92 ± 0.04	0.93 ± 0.02

S denotes sham group, 5 denotes 5-minute tDCS, and 15 denotes 15-minute tDCS. The values are presented as the mean ± standard deviation.

it was observed that the degree of the C3 node in the beta band and the average clustering coefficients of brain regions showed significant associations with tDCS. This finding aligns with previous research [48] that established the relationship between the beta band EEG signal and muscle contraction. The establishment of functional beta-band oscillatory synchronization between the primary motor cortex (M1) and spinal motor neurons innervating actively engaged muscles serves as a pivotal determinant in the regulation of motor control [49,50]. The synchronization of oscillatory brain activities can be quantified through the coherence analysis of EEG and EMG signals. This approach serves as an established metric for assessing the integrity of the pyramidal system referred to as corticomuscular coherence (CMC) [51]. Alterations in CMC have been observed subsequent to the acquisition of novel motor skills among healthy individuals, which has demonstrated that the augmentation of CMC is linked with functional motor recovery in stroke patients [52]. These studies show that the signals of EEG and EMG are closely connected, indicating that the human body's motor function is complete.

In the experiment, it was found that the results of the 15-minute stimulation of P3 and F3 nodes were significantly different from those of the 5-minute stimulation. Compared with before stimulation, the results of the 5-minute stimulation of the P3 node were not significant, but the results of the 15-minute stimulation were significant. This shows that increasing the stimulation duration of tDCS may increase the range of brain areas affected.

The degree of the C3 node increased significantly after tDCS, which may indicate that the cortical area issued stronger control commands to the corresponding limbs [53]. At the same time, the changes in average clustering coefficients indicate that the information interaction of each area of the cortex is more frequent [54], which may include information from the state of muscle movement. In summary, the role of tDCS is likely to strengthen the cortex to send control commands to the muscles, and the state information of the muscles is transmitted to the cortex, such as a closed-loop control pathway. These two characteristic parameters may be used to partially explain the results of muscle synergy activation matrix H changes when the participant's hand movement after tDCS stimulation; that is, tDCS enhanced the C3 node and its surrounding areas.

A study [55] has pointed out that muscle activity mainly results from cortical projections. On the other hand, the motor cortex control and sensory functions of stroke patients are lost or disordered, and motor dysfunction, such as abnormal muscle tone, occurs. The theory [56] of neuroplasticity points out that for patients with a damaged central nervous system, taking timely and reasonable autonomous rehabilitation treatment can change the shape of nerve tissue or reconstruct the motor nerve pathway compensatory-ly so that the motor function can be restored to a certain extent. In other words, as long as it can only enhance the connection between cortical activity and muscles, it may be very helpful for rehabilitation exercises.

Although this study compared only the two tDCS durations of 5 minutes and 15 minutes, further investigation is necessary to establish a more precise relationship curve between tDCS duration and its effect on muscle synergy, as well as the duration of this effect. In addition, the number of volunteers in the experiment can be increased. In order to study the stimulus position more accurately, tDCS equipment with higher position resolution (High-Definition Transcranial Direct Current Stimulation, HD-tDCS) can be used.

5. Conclusions

In this experiment, it can be seen that the cortical activity of the brain area impacts the corresponding muscles involved in hand movement; tDCS is anticipated to enhance cortical functionality for transmitting control commands to the musculature while simultaneously facilitating the conveyance of muscular state information back to the cortex. Duration of tDCS may broaden the scope of cerebral regions influenced by the stimulation. Thereby not only corroborating the promotion effect of tDCS on motor enhancement but also demonstrating the potential of tDCS in sports rehabilitation.

Availability of Data and Materials

The datasets used or analysed during the current study are available from the corresponding author on reasonable request.

Author Contributions

ZL and SC designed the research study. SC performed the research and wrote the manuscript. JL conducted a literature review and analyze data. All authors contributed to editorial changes in the manuscript. All authors read and approved the final manuscript. All authors have participated sufficiently in the work and agreed to be accountable for all aspects of the work.

Ethics Approval and Consent to Participate

The study was in accordance with the Declaration of Helsinki (1964). Written, informed consent was obtained from all participants before inclusion in the study, and the protocol was approved by the medical ethics committee of Zhejiang Hospital (approval number: No. 20230010K).

Acknowledgment

Not applicable.

Funding

The National Natural Science Foundation of China (No. 62171171). The key project of Zhejiang Provincial Natural Science Foundation (LZ23F030005).

Conflict of Interest

The authors declare no conflict of interest.

References

[1] Virani SS, Alonso A, Aparicio HJ, Benjamin EJ, Bittencourt MS, Callaway CW, *et al*. Heart Disease and Stroke Statistics-2021 Update: A Report From the American Heart Association. Circulation. 2021; 143: e254–e743.

[2] Kim RK, Kang N. Bimanual Coordination Functions between Paretic and Nonparetic Arms: A Systematic Review and Meta-analysis. Journal of Stroke and Cerebrovascular Diseases. 2020; 29: 104544.

[3] Starosta M, Cichoń N, Saluk-Bijak J, Miller E. Benefits from Repetitive Transcranial Magnetic Stimulation in Post-Stroke Rehabilitation. Journal of Clinical Medicine. 2022; 11: 2149.

[4] Priori A, Hallett M, Rothwell JC. Repetitive transcranial magnetic stimulation or transcranial direct current stimulation? Brain Stimulation. 2009; 2: 241–245.

[5] Lauro LJR, Rosanova M, Mattavelli G, Convento S, Pisoni A, Opitz A, *et al*. TDCS increases cortical excitability: Direct evidence from TMS–EEG. Cortex. 2014; 58: 99–111.

[6] de Araújo AVL, Ribeiro FPG, Massetti T, Potter-Baker KA, Cortes M, Plow EB, *et al*. Effectiveness of anodal transcranial direct current stimulation to improve muscle strength and motor functionality after incomplete spinal cord injury: a systematic review and meta-analysis. Spinal Cord. 2020; 58: 635–646.

[7] Nitsche MA, Paulus W. Excitability changes induced in the human motor cortex by weak transcranial direct current stimulation. The Journal of Physiology. 2000; 527: 633–639.

[8] Das S, Holland P, Frens MA, Donchin O. Impact of Transcranial Direct Current Stimulation (tDCS) on Neuronal Functions. Frontiers in Neuroscience. 2016; 10: 550.

[9] Nikolin S, Huggins C, Martin D, Alonzo A, Loo CK. Safety of repeated sessions of transcranial direct current stimulation: A systematic review. Brain Stimulation. 2018; 11: 278–288.

[10] Bikson M, Grossman P, Thomas C, Zannou AL, Jiang J, Adnan T, *et al*. Safety of Transcranial Direct Current Stimulation: Evidence Based Update 2016. Brain Stimulation. 2016; 9: 641–661.
[11] Zaghi S, Acar M, Hultgren B, Boggio PS, Fregni F. Noninvasive brain stimulation with low-intensity electrical currents: putative mechanisms of action for direct and alternating current stimulation. The Neuroscientist. 2010; 16: 285–307.
[12] Molero-Chamizo A, Alameda Bailén JR, Garrido Béjar T, García López M, Jaén Rodríguez I, Gutiérrez Lérida C, *et al*. Post-stimulation time interval-dependent effects of motor cortex anodal tDCS on reaction-time task performance. Cognitive, Affective & Behavioral Neuroscience. 2018; 18: 167–175.
[13] Miranda PC. Physics of effects of transcranial brain stimulation. Handbook of Clinical Neurology. 2013; 116: 353–366.
[14] Reis J, Schambra HM, Cohen LG, Buch ER, Fritsch B, Zarahn E, *et al*. Noninvasive cortical stimulation enhances motor skill acquisition over multiple days through an effect on consolidation. Proceedings of the National Academy of Sciences of the United States of America. 2009; 106: 1590–1595.
[15] Liu X, Yang X, Hou Z, Ma M, Jiang W, Wang C, *et al*. Increased interhemispheric synchrony underlying the improved athletic performance of rowing athletes by transcranial direct current stimulation. Brain Imaging and Behavior. 2019; 13: 1324–1332.
[16] Hazime FA, da Cunha RA, Soliaman RR, Romancini ACB, Pochini ADC, Ejnisman B, *et al*. Anodal transcranial direct current stimulation (tdcs) increases isometric strength of shoulder rotators muscles in handball players. International Journal of Sports Physical Therapy. 2017; 12: 402–407.
[17] Alisar DC, Ozen S, Sozay S. Effects of Bihemispheric Transcranial Direct Current Stimulation on Upper Extremity Function in Stroke Patients: A randomized Double-Blind Sham-Controlled Study. Journal of Stroke and Cerebrovascular Diseases. 2020; 29: 104454.
[18] Bolognini N, Russo C, Souza Carneiro MI, Nicotra A, Olgiati E, Spandri V, *et al*. Bi-hemispheric transcranial direct current stimulation for upper-limb hemiparesis in acute stroke: a randomized, double-blind, sham-controlled trial. European Journal of Neurology. 2020; 27: 2473–2482.
[19] Bornheim S, Thibaut A, Beaudart C, Maquet P, Croisier JL, Kaux JF. Evaluating the effects of tDCS in stroke patients using functional outcomes: a systematic review. Disability and Rehabilitation. 2022; 44: 13–23.
[20] Gladstone DJ, Danells CJ, Black SE. The fugl-meyer assessment of motor recovery after stroke: a critical review of its measurement properties. Neurorehabilitation and Neural Repair. 2002; 16: 232–240.
[21] Hsu SP, Lu CF, Lin BF, Tang CW, Kuo IJ, Tsai YA, *et al*. Effects of bihemispheric transcranial direct current stimulation on motor recovery in subacute stroke patients: a double-blind, randomized sham-controlled trial. Journal of Neuroengineering and Rehabilitation. 2023; 20: 27.
[22] Kashoo FZ, Al-Baradie RS, Alzahrani M, Alanazi A, Manzar MD, Gugnani A, *et al*. Effect of Transcranial Direct Current Stimulation Augmented with Motor Imagery and Upper-Limb Functional Training for Upper-Limb Stroke Rehabilitation: A Prospective Randomized Controlled Trial. International Journal of Environmental Research and Public Health. 2022; 19: 15199.
[23] Zhou C, Zemanová L, Zamora G, Hilgetag CC, Kurths J. Hierarchical organization unveiled by functional connectivity in complex brain networks. Physical Review Letters. 2006; 97: 238103.
[24] Safavynia SA, Torres-Oviedo G, Ting LH. Muscle Synergies: Implications for Clinical Evaluation and Rehabilitation of Movement. Topics in Spinal Cord Injury Rehabilitation. 2011; 17: 16–24.
[25] Beuchat NJ, Chavarriaga R, Degallier S, Millán JDR. Offline decoding of upper limb muscle synergies from EEG slow cortical potentials. Annual International Conference of the IEEE Engineering in Medicine and Biology Society. IEEE Engineering in Medicine and Biology Society. Annual International Conference. 2013; 2013: 3594–3597.
[26] Yokoyama H, Kaneko N, Ogawa T, Kawashima N, Watanabe K, Nakazawa K. Cortical Correlates of Locomotor Muscle Synergy Activation in Humans: An Electroencephalographic Decoding Study. iScience. 2019; 15: 623–639.
[27] Morya E, Monte-Silva K, Bikson M, Esmaeilpour Z, Biazoli CE, Jr, Fonseca A, *et al*. Beyond the target area: an integrative view of tDCS-induced motor cortex modulation in patients and athletes. Journal of Neuroengineering and Rehabilitation. 2019; 16: 141.
[28] Oldfield RC. Edinburgh handedness inventory. Journal of Abnormal Psychology. 1971.
[29] Chen Y, Akutagawa M, Katayama M, Zhang Q, Kinouchi Y. ICA based multiple brain sources localization. Annual International Conference of the IEEE Engineering in Medicine and Biology Society. IEEE Engineering in Medicine and Biology Society. Annual International Conference. 2008; 2008: 1879–1882.
[30] Crespo-Garcia M, Atienza M, Cantero JL. Muscle artifact removal from human sleep EEG by using independent component analysis. Annals of Biomedical Engineering. 2008; 36: 467–475.
[31] Jung TP, Makeig S, Westerfield M, Townsend J, Courchesne E, Sejnowski TJ. Removal of eye activity artifacts from visual event-related potentials in normal and clinical subjects. Clinical Neurophysiology. 2000; 111: 1745–1758.
[32] Delorme A, Palmer J, Onton J, Oostenveld R, Makeig S. Independent EEG sources are dipolar. PLoS ONE. 2012; 7: e30135.
[33] Leutheuser H, Gabsteiger F, Hebenstreit F, Reis P, Lochmann M, Eskofier B. Comparison of the AMICA and the InfoMax algorithm for the reduction of electromyogenic artifacts in EEG data. Annual International Conference of the IEEE Engineering in Medicine and Biology Society. IEEE Engineering in Medicine and Biology Society. Annual International Conference. 2013; 2013: 6804–6807.
[34] Palmer JA, Kreutz-Delgado K, Makeig S. AMICA: An adaptive mixture of independent component analyzers with shared components. Swartz Center for Computatonal Neursoscience, University of California San Diego, Tech. Rep. 2012; 1–15.
[35] Pion-Tonachini L, Kreutz-Delgado K, Makeig S. ICLabel: An automated electroencephalographic independent component classifier, dataset, and website. NeuroImage. 2019; 198: 181–197.
[36] Monachino AD, Lopez KL, Pierce LJ, Gabard-Durnam LJ. The HAPPE plus Event-Related (HAPPE+ER) software: A standardized preprocessing pipeline for event-related potential analyses. Developmental Cognitive Neuroscience. 2022; 57: 101140.
[37] Delorme A. EEG is better left alone. Scientific Reports. 2023; 13: 2372.
[38] Hjorth B. The physical significance of time domain descriptors in EEG analysis. Electroencephalography and Clinical Neurophysiology. 1973; 34: 321–325.
[39] Liu M, Xu G, Yu H, Wang C, Sun C, Guo L. Effects of Transcranial Direct Current Stimulation on EEG Power and Brain Functional Network in Stroke Patients. IEEE Transactions on Neural Systems and Rehabilitation Engineering. 2023; 31: 335–345.
[40] Bizzi E, Cheung VCK. The neural origin of muscle synergies. Frontiers in Computational Neuroscience. 2013; 7: 51.
[41] Bernstein N. The co-ordination and regulation of movements. Pergamon Press: Oxford, UK. 1967.
[42] Wang YX, Zhang YJ. Nonnegative matrix factorization: A com-

prehensive review. IEEE Transactions on Knowledge and Data Engineering. 2012; 25: 1336–1353.
[43] Tresch MC, Cheung VCK, d'Avella A. Matrix factorization algorithms for the identification of muscle synergies: evaluation on simulated and experimental data sets. Journal of Neurophysiology. 2006; 95: 2199–2212.
[44] Frère J, Hug F. Between-subject variability of muscle synergies during a complex motor skill. Frontiers in Computational Neuroscience. 2012; 6: 99.
[45] Scotto di Luzio F, Cordella F, Bravi M, Santacaterina F, Bressi F, Sterzi S, *et al*. Modification of hand muscular synergies in stroke patients after robot-aided rehabilitation. Applied Sciences. 2022; 12: 3146.
[46] Benjamini Y, Yekutieli D. The control of the false discovery rate in multiple testing under dependency. Annals of Statistics. 2001: 1165–1188.
[47] Chintakindi SR, Varaprasad O, Sarma DS. Improved Hanning window based interpolated FFT for power harmonic analysis. TENCON 2015-2015 IEEE Region 10 Conference. IEEE. 2015: 1–5.
[48] Brovelli A, Ding M, Ledberg A, Chen Y, Nakamura R, Bressler SL. Beta oscillations in a large-scale sensorimotor cortical network: directional influences revealed by Granger causality. Proceedings of the National Academy of Sciences of the United States of America. 2004; 101: 9849–9854.
[49] Perez MA, Lundbye-Jensen J, Nielsen JB. Changes in corticospinal drive to spinal motoneurones following visuo-motor skill learning in humans. The Journal of Physiology. 2006; 573: 843–855.
[50] Yamaguchi T, Svane C, Forman CR, Beck MM, Geertsen SS, Lundbye-Jensen J, *et al*. Transcranial Alternating Current Stimulation of the Primary Motor Cortex after Skill Acquisition Improves Motor Memory Retention in Humans: A Double-Blinded Sham-Controlled Study. Cerebral Cortex Communications. 2020; 1: tgaa047.
[51] Mima T, Hallett M. Corticomuscular coherence: a review. Journal of Clinical Neurophysiology. 1999; 16: 501–511.
[52] Krauth R, Schwertner J, Vogt S, Lindquist S, Sailer M, Sickert A, *et al*. Cortico-Muscular Coherence Is Reduced Acutely Post-stroke and Increases Bilaterally During Motor Recovery: A Pilot Study. Frontiers in Neurology. 2019; 10: 126.
[53] Willems RM, Ozyürek A, Hagoort P. Differential roles for left inferior frontal and superior temporal cortex in multimodal integration of action and language. NeuroImage. 2009; 47: 1992–2004.
[54] Latora V, Marchiori M. Efficient behavior of small-world networks. Physical Review Letters. 2001; 87: 198701.
[55] Bräcklein M, Barsakcioglu DY, Del Vecchio A, Ibáñez J, Farina D. Reading and Modulating Cortical β Bursts from Motor Unit Spiking Activity. The Journal of Neuroscience. 2022; 42: 3611–3621.
[56] Sanes JN, Donoghue JP. Plasticity and primary motor cortex. Annual Review of Neuroscience. 2000; 23: 393–415.